Dielectric properties of interacting storage ring plasmas

A. Selchow and K. Morawetz
Fachbereich Physik, Universität Rostock, D-18051 Rostock, Germany
(Received 5 June 1998)

A dielectric function (DF) including collisional correlations is derived by linearizing the self-consistent Vlasov equation with a Fokker-Planck collision integral. The calculation yields the same type of dielectric function as in the standard theory of Schottky noise in storage rings. This dielectric function is compared with the Mermin dielectric function derived from a kinetic equation with a relaxation-time approximation. We observe that these functions are identical, however the Mermin DF is computationally advantageous. The limits of both dielectric functions are given and the sum rules are proven. We apply these dielectric functions for typical storage ring plasmas and calculate the stopping power and the plasmon excitation spectrum.
[S1063-651X(98)13612-7]

PACS number(s): 52.25.Wz, 41.75.Ak, 52.20.−j, 52.40.Mj

I. INTRODUCTION

During the past ten years experiments with ions (p^+ up to U^{92+}) in storage rings gained importance in the field of spectroscopy and plasma physics. The stored and cooled ion beams have a high luminosity for recombination experiments and inertial confined fusion investigations. In particular, it is of basic interest to study the transition between the weak and strong coupled plasma or even the transition to a crystalline state of a cooled ion beam [1]. The most important prerequisite for obtaining dense states is strong electron and laser cooling. The electron cooling force can be described as stopping power acting on an ion beam in an electron plasma [2]. Other plasma phenomena in dense beams are collective excitations (plasmons, shear modes) which are detectable by the Schottky noise [3]. All items—the pair distribution function of a state, the stopping power, and the shape of the collective excitations—are related to the dielectric function (DF) $\epsilon(\vec{q},\omega)$.

Within the linear-response theory the polarizability $\Pi(\vec{q},\omega)$ [and altogether the dielectric function $\epsilon(\vec{q},\omega)$] is defined by the variation of particle density $\delta n(\vec{q},\omega)$ in reaction to an external field $\delta U_{\rm ext}(\vec{q},\omega)$ via

$$\Pi(\vec{q},\omega)=\frac{\delta n(\vec{q},\omega)}{\delta U_{\rm ext}}. \tag{1}$$

The connection to the dielectric function (DF) is given by

$$\epsilon(\vec{q},\omega)=1+V_C(\vec{q})\Pi(\vec{q},\omega). \tag{2}$$

The captured ions in storage rings are moving in front of a background of the confining fields ensuring approximately the charge neutrality in the system. This nearly neutral system of ions interacting via the Coulomb potential V_C immersed in a homogeneous background of opposite charge is usually called a one-component plasma (OCP).

An unpleasant problem is the temperature anisotropy. The longitudinal temperature ($T_\parallel$) differs from the transversal ($T_\perp$) (referring to the beam axis) because only the longitudinal direction is cooled directly. Even taking into account relaxation processes between the degrees of freedom and possible transversal cooling, the temperature difference is maintained.

In this paper we focus on experiments done by the Heidelberg TSR group with $^9Be^+$ and $^{12}C^{6+}$ ions cooled by an electron beam [1,4]. The $^9Be^+$ ions can be cooled further down to a few mK by applying laser cooling (see Table I).

For estimations about the ideality and collision numbers, we employ the longitudinal temperature $T_\parallel$. The density of the ion beam can be calculated using the current j of the beam profile (the diameter) measured by the beam profile monitors $x_{\rm BPM}$ and the value of the betatron function on this position $\beta_{\rm BPM}$,

$$n=\frac{jQ\beta_{\rm BPM}}{2\pi Z x_{\rm BPM}^2 R v_0}. \tag{3}$$

Here v_0 denotes the ion beam velocity, R is the ring radius, and Z is the charge state of the ions. The transversal tune Q amounts to 2.8.

The essential parameter for characterizing the coupling is the nonideality or plasma parameter

$$\Gamma=\frac{e^2}{4\pi\epsilon_0 k_B T}\left(\frac{4\pi n}{3}\right)^{1/3} \tag{4}$$

which is the ratio of the potential and thermal energy. Further essential quantities are the plasma frequency

TABLE I. Parameters for several experiments in the TSR. The explanations are given in the text. Data are from [1,4].

Parameter	Be^+	C^{6+}	e^-
n	2.3×10^{13} m^{-3}	1.6×10^{13} m^{-3}	2.9×10^{13} m^{-3}
$T_\parallel$	6 K	8000 K	3.5 K
Γ	0.13	0.0031	0.23
λ	1.7×10^{7} s^{-1}	4.0×10^{5} s^{-1}	3.4×10^{12} s^{-1}
$\omega_{\rm pl}$	2.1×10^{6} s^{-1}	9.2×10^{6} s^{-1}	3.0×10^{8} s^{-1}

 ©1999 The American Physical Society

$$\omega_{\rm pl}=\sqrt{\frac{ne^2}{\epsilon_0 m}} \tag{5}$$

and the inverse screening length

$$\kappa=\sqrt{\frac{ne^2}{\epsilon_0 k_B T}}\,. \tag{6}$$

Another important parameter characterizing the plasma is the collision frequency, or friction coefficient λ, which is the inverse relaxation time

$$\begin{aligned}\lambda&=\frac{1}{\tau}=n\sigma(v_{\rm th})v_{\rm th},\\ \sigma(v)&=4\pi\left(\frac{2e^2}{12\epsilon_0 k_B T}\right)\Lambda(v).\end{aligned} \tag{7}$$

Here $\sigma(v_{th})$ is the cross section at thermal velocity $v_{\rm th}^2=2k_BT/m$ for ion-ion collisions and $\Lambda(v)$ denotes the Coulomb logarithm, e.g., in the Brooks-Herring approximation.

The collisions between the ions play an essential role in this storage ring plasmas, being responsible for effects such as intrabeam scattering (IBS) [5]. That means an expansion of the (ion) beam due to ion-ion collisions has to be suppressed by electron cooling. Consequently, for a more complete description a dielectric function $\epsilon(\vec{q},\omega)$ including these collisions should be considered [6]. In this paper two practical methods will be shown in Sec. II.

An essential property of every dielectric function is the fulfillment of the sum rules. The strongest are the longitudinal frequency sum rule

$$\int_0^\infty \frac{2\omega}{\pi\omega_{\rm pl}^2}{\rm Im}\ \epsilon^{-1}(\vec{q},\omega)d\omega=1 \tag{8}$$

and the conductivity sum rule

$$\int_0^\infty \frac{2\omega}{\pi\omega_{\rm pl}^2}{\rm Im}\ \epsilon(\vec{q},\omega)d\omega=-1; \tag{9}$$

moreover, the compressibility sum rule

$$\lim_{q\to 0}\int_0^\infty \frac{2}{\pi\omega_{\rm pl}^2}\frac{1}{\omega}{\rm Im}\ \epsilon^{-1}(\vec{q},\omega)d\omega=1 \tag{10}$$

and the perfect screening sum rule

$$\lim_{q\to 0}\int_0^\infty \frac{2}{\pi\omega_{\rm pl}^2}\frac{1}{\omega}{\rm Im}\ \epsilon(\vec{q},\omega)d\omega=-1. \tag{11}$$

The validity of these sum rules is an essential statement about the quality and reliability of the dielectric function.

The outline of the paper is as follows. In Sec. II A we give a short rederivation of the Mermin DF, and the DF from a Fokker-Planck equation is given in Sec. II B. In Sec. II C we compare both DF's, and the sum rules are proven in Sec. II D. In Sec. III A we present the application to the stopping power and in Sec. III B we calculate the Schottky spectra.

II. DIELECTRIC FUNCTIONS WITH CORRELATIONS

A. Mermin dielectric function

For calculating a dielectric function including collisions between the particles with mass m, Mermin [7] suggested a particle number conserving dielectric function. We briefly sketch his derivation for the classical case starting with a kinetic equation in the relaxation-time approximation,

$$\begin{aligned}&\frac{\partial}{\partial t}f(\vec{r},\vec{v},t)+\vec{v}\frac{\partial}{\partial\vec{r}}f(\vec{r},\vec{v},t)+\frac{\partial}{\partial\vec{r}}\frac{U(\vec{r},t)}{m}\frac{\partial}{\partial\vec{v}}f(\vec{r},\vec{v},t)\\ &\quad=-\frac{f(\vec{r},\vec{v},t)-f_0(\vec{v})}{\tau}.\end{aligned} \tag{12}$$

This kinetic equation describes the development of a particle distribution function $f(\vec{r},\vec{v},t)$ consisting of an equilibrium part $f_0(\vec{v})$ and a nonequilibrium part $\delta f(\vec{r},\vec{v},t)$

$$f(\vec{r},\vec{v},t)=f_0(\vec{v})+\delta f(\vec{r},\vec{v},t). \tag{13}$$

The mean field $U(\vec{r},t)$ is composed of an external part and a part arising from the induced particle density δn,

$$U(\vec{q},\omega)=\delta U_{\rm ext}+V\delta n(\vec{q},\omega). \tag{14}$$

One gets the induced particle density δn by linearization of Eq. (12) and integrating the solution of δf over the velocity $\vec{v}$. After Fourier transformation $t\to\omega$ and $r\to q$ the following polarization function $\Pi(\vec{q},\omega)$ is obtained:

$$\begin{aligned}\delta n(\vec{q},\omega)&=\int \delta f(\vec{q},\vec{v},\omega)d^3v\\ &=\frac{\Pi_0(\vec{q},\omega+i/\tau)}{1-V(\vec{q})\Pi_0(\vec{q},\omega+i/\tau)}\delta U_{\rm ext}(\vec{q},\omega)\end{aligned} \tag{15}$$

with the RPA or Lindhard polarization function

$$\Pi_0(\vec{q},\omega)=\int d^3v\frac{\frac{\vec{q}}{m}\frac{\partial}{\partial\vec{v}}f(\vec{v})}{\vec{v}\vec{q}-\omega+i/\tau}. \tag{16}$$

The RPA dielectric function (2) in the classical limit reads

$$\begin{aligned}\epsilon(q,\omega)&=1+\frac{\kappa^2}{q^2}\left(1-2x_c e^{-x_c^2}\int_0^{x_c}e^{t^2}dt+i\sqrt{\pi}x_c e^{-x_c^2}\right),\\ x_c&=\sqrt{\frac{m}{2k_BT}}\frac{\omega}{q},\end{aligned} \tag{17}$$

and fulfills all sum rules (8)–(11). Shifting the frequency into the complex plane according to Eq. (16), one gets the relaxation dielectric function. This expression does not fulfill the limit of static screening and has a non-Drude-like high-frequency behavior which leads to a violation of the sum rules (8)–(11).

In [7] a more sophisticated dielectric function was suggested by considering the relaxation ansatz

$$\frac{\partial}{\partial t}f(\vec{r},\vec{v},t)+\vec{v}\frac{\partial}{\partial \vec{r}}f(\vec{r},\vec{v},t)+\frac{\partial}{\partial \vec{r}}\frac{U(\vec{r},t)}{m}\frac{\partial}{\partial \vec{v}}f(\vec{r},\vec{v},t)$$
$$=-\frac{f(\vec{r},\vec{v},t)-\tilde{f}_0(\vec{r},\vec{v},t)}{\tau}. \tag{18}$$

with respect to a local equilibrium distribution function

$$\tilde{f}_0(\vec{r},\vec{v},t)=\exp\left[-\frac{mv^2}{2k_BT}+\frac{\mu+\delta\mu(\vec{r},t)}{k_BT}\right] \tag{19}$$

instead of the global distribution $f_0(\vec{v})$ in Eq. (12). In the simplest case one can specify the local distribution by a small fluctuation in the chemical potential $\delta\mu$ related to the density fluctuation δn.

The Mermin dielectric function is derived by solving Eq. (18) using an expansion of the local equilibrium distribution function in powers of $\delta\mu$,

$$\tilde{f}_0(\vec{q},\vec{v},\omega)=f_0(\vec{v})-\frac{\vec{q}\vec{\partial}_v f_0(\vec{v})}{m\vec{q}\vec{v}}\delta\mu(\vec{q},\omega), \tag{20}$$

where $\delta\mu$ is determined by the particle number conservation $\omega\delta n(\vec{q},\omega)=\int\vec{v}\vec{q}\,\delta f(\vec{q},\vec{v},\omega)d^3v$ leading to [7]

$$\delta\mu(\vec{q},\omega)=\frac{\delta n(\vec{q},\omega)}{\Pi(\vec{q},0)}. \tag{21}$$

Finally one obtains from Eqs. (18) and (20) for the polarization function

$$\Pi_{\mathrm{M}}(\vec{q},\omega)=\frac{\Pi_0(\vec{q},\omega+i/\tau)}{1-\frac{1}{1-i\omega\tau}\left(1-\frac{\Pi_0(\vec{q},\omega+i/\tau)}{\Pi_0(\vec{q},0)}\right)}. \tag{22}$$

Instead of Eq. (15) we arrive at a density variation

$$\delta n(\vec{q},\omega)=\frac{\Pi_{\mathrm{M}}(\vec{q},\omega+i/\tau)}{1-V(\vec{q})\Pi_{\mathrm{M}}(\vec{q},\omega+i/\tau)}\delta U_{\mathrm{ext}}(\vec{q},\omega) \tag{23}$$

and with Eq. (2) the Mermin dielectric function finally has the shape

$$\epsilon_{\mathrm{M}}\left(\vec{q},\omega+\frac{i}{\tau}\right)=1+\frac{[1+i/(\omega\tau)][\epsilon(\vec{q},\omega+i/\tau)-1]}{1+\frac{i}{\omega\tau}\frac{\epsilon(\vec{q},\omega+i/\tau)-1}{\epsilon(\vec{q},0)-1}}. \tag{24}$$

Here $\epsilon(\vec{q},\omega+i/\tau)$ denotes the dielectric function (17) in the relaxation-time approximation. It is easy to see that in the limit $\tau\to\infty$, the Mermin dielectric function reproduces the RPA dielectric function (17) in the classical limit. Here we can restrict ourselves to the classical case for the polarization function. The original Mermin result is given by the quantum RPA dielectric function.

B. The Vlasov-Fokker-Planck equation (VFP equation)

Now we examine another kinetic equation—the Vlasov equation with the Fokker-Planck collision integral which has been used to predict the Schottky noise of an ion beam [3],

$$\frac{\partial}{\partial t}f(\vec{r},\vec{v},t)+\vec{v}\frac{\partial}{\partial \vec{r}}f(\vec{r},\vec{v},t)+\frac{\partial}{\partial \vec{r}}\frac{U(\vec{r},t)}{m}\frac{\partial}{\partial \vec{v}}f(\vec{r},\vec{v},t)$$
$$=\lambda\frac{\partial}{\partial\vec{v}}\left(\frac{D}{\lambda}\frac{\partial}{\partial\vec{v}}+\vec{v}\right)f(\vec{r},\vec{v},t). \tag{25}$$

The application of the Fokker-Planck collision term is valid for weak collisions (it means low q values) because it represents an expansion of the collision integral in momentum space. With the collision integral of the Fokker-Planck equation one includes the fluctuations of the distribution function due to collisions. It describes the balance between dynamical friction $\lambda(\partial/\partial\vec{v})(\vec{v}f(\vec{r},\vec{v},t))$ holding the velocity distribution sharply near zero velocity and the diffusion $D(\partial^2/\partial v^2)f(\vec{r},\vec{v},t)$ flattening the velocity distribution. The coefficients λ and D in the Fokker-Planck equation are related by the Einstein relation

$$\frac{D}{\lambda}=\frac{k_BT}{m}. \tag{26}$$

As already mentioned above, the friction coefficient λ is equal to the inverse relaxation time. Obviously, the drift coefficient $\lambda\vec{v}$ is linear in the velocity as long as the diffusion coefficient D is a constant. The Fokker-Planck collision term ensures the particle conservation. Due to the Einstein relation we have a proper balance between friction and diffusion. So we expect that physics is included similar to the Mermin extension of the simple relaxation-time approximation in the preceding paragraph.

We solve this Fokker-Planck equation again within the linear response. A sketch of the derivation can be found in Appendix A with the result for the dielectric function

$$\epsilon_{\mathrm{VFP}}(q,\omega)=1+\frac{\kappa^2}{q^2}\left[1+\frac{i\omega}{\frac{k_BT}{m}\frac{q^2}{\lambda}-i\omega}{}_1F_1\left(1,1+\frac{k_BT}{m\lambda^2}q^2-i\frac{\omega}{\lambda};\frac{k_BT}{m\lambda^2}q^2\right)\right] \tag{27}$$

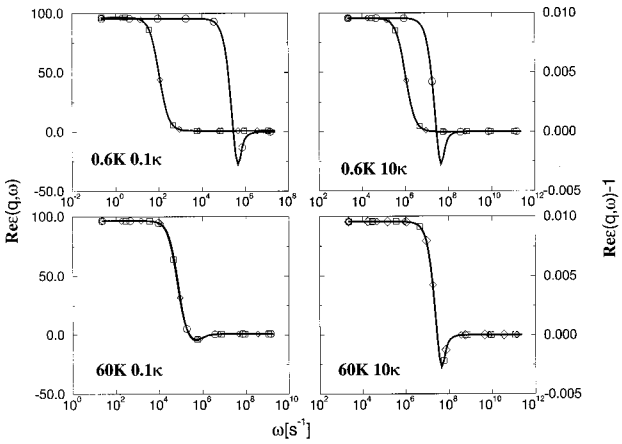

FIG. 1. Comparison of the real parts of the RPA (circles), Mermin (squares), and VFP dielectric function (diamonds). We have chosen temperatures of 0.6–60 K available in the longitudinal direction of an ion beam and wave numbers below and above the inverse Debye length κ (6). The particle density is $n=2.3\times10^{13}$ m^{-3} of single charged beryllium ions. The real parts of Mermin and the VFP DF are identical.

and ${}_1F_1$ denotes the confluent hypergeometric function. This dielectric function has been given in [3] and is valid for an isotropic plasma in three dimensions.

C. Comparison of both dielectric functions

Up to now we have used different kinetic equations leading to two different dielectric functions. It is of great interest how these functions are related to each other and whether these dielectric functions are valid in the storage ring plasma's realm of temperature, density, and friction coefficient. In Figs. 1 and 2 both dielectric functions are plotted in dependence on the frequency for several wave numbers and temperatures.

We see that within the numerical accuracy of the picture no difference is visible between the dielectric function of a Fokker-Planck collision integral and the Mermin dielectric

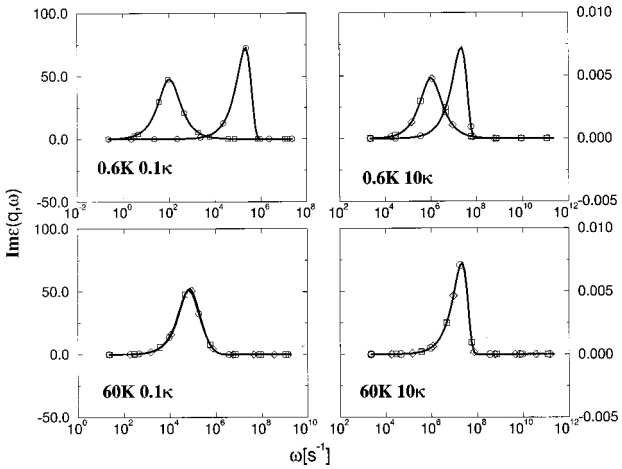

FIG. 2. Comparison of the imaginary parts of the RPA (circles), Mermin (squares), and VFP DF (diamonds). The same density and temperatures are chosen as in Fig. 1. The imaginary parts of Mermin and the VFP DF are identical.

function resulting from the conserving relaxation-time approximation.

Let us inspect now some special limits. Both dielectric functions fulfill the static limit ($\omega\to0$)

$$\epsilon(q,0)=1+\frac{\kappa^2}{q^2} \tag{28}$$

for all λ in accordance with the classical Debye-Hückel result for static screening. In the long-wavelength limit $q\to0$ one gets the Drude formula for both dielectric functions

$$\lim_{\substack{q\to0\\ \omega\to\infty}}\epsilon(q,\omega)=1-\frac{\omega_{\rm pl}^2}{\omega(\omega+i\lambda)}. \tag{29}$$

For $\lambda\to0$ this formula reproduces the RPA behavior. In the limit of strong friction $\lambda\to\infty$ we get in agreement with [3] and [8] also Eq. (29). The long-wavelength and the strong friction limits are identical.

For low temperatures there are differences between the RPA dielectric function and the other correlated dielectric functions. The real parts start in the static limit at the same value as the RPA dielectric function but drop down much earlier (in Fig. 1 one sees four orders of magnitude at one-tenth of the inverse Debye length and two orders of magnitude at ten times the inverse Debye length). There are no zeros in the real part. Accordingly, the imaginary part is shifted in the same fashion. It is one magnitude broader than the RPA imaginary part and has only two-thirds of its height. For temperatures higher than 50 K the RPA dielectric function and the Mermin and VFP dielectric functions become identical.

D. Sum rules

The most interesting question is whether the dielectric function fulfills the sum rules (8)–(11). Due to Eq. (29) all presented dielectric functions lead to Re $\epsilon(\vec{q},\omega)\propto\omega^{-2}$ for large ω. Since poles due to the relaxation time occur only in the lower half plane we have

$$\int_{-\infty}^{\infty}d\bar{\omega}\frac{\epsilon^{-1}(\vec{q},\bar{\omega})-1}{(\bar{\omega}+i\eta)}=0 \tag{30}$$

from which we see that the dielectric functions fulfill the Kramers-Kronig relations

$$\mathrm{Re}\ \epsilon^{-1}(\vec{q},\omega)-1=\mathrm{P}\int_{-\infty}^{\infty}\frac{2\ \mathrm{Im}\ \epsilon^{-1}(\vec{q},\bar{\omega})}{\omega-\bar{\omega}}\frac{d\bar{\omega}}{2\pi} \tag{31}$$

where the P denotes here the Cauchy principle value.

From Eq. (31) we get with Eq. (28) in the static limit just the compressibility sum rule (10). The longitudinal *f*-sum rule (8) follows as well from Eq. (31). To see this we observe that due to time reversibility $\epsilon(q,-\omega)=\epsilon^*(q,\omega)$ holds and we can write

$$\lim_{\omega\to\infty}\mathrm{Re}\ \epsilon^{-1}(q,\omega)=1+\lim_{\omega\to\infty}\frac{2}{\omega^2\pi}\int_0^{\infty}d\bar{\omega}\ \mathrm{Im}\ \epsilon^{-1}(q,\bar{\omega}). \tag{32}$$

Using Eq. (29) we obtain just the *f*-sum rule (8).

Since the same Kramers-Kronig relation (31) holds also for ϵ instead of ϵ^{-1}, we see that the corresponding free sum rules (9) and (11) are also fulfilled.

This completes the proof that both correlated dielectric functions fulfill the sum rules. We can state, therefore, that both dielectric functions are properly valid in the interesting scope and can be used to describe the phenomena in cold and dilute storage ring plasmas. Since the Mermin dielectric function is computationally much easier to handle than the VFP DF, we will use the Mermin dielectric function further on.

III. APPLICATION TO STORAGE RING PLASMAS

We continue now to apply the correlated dielectric function derived in the preceding paragraph to typical storage ring plasmas. We would like to discuss two important quantities here: the stopping power of ions in an electron plasma and the occurring plasmon excitations.

A. Stopping power

The stopping power, i.e., the energy transfer of a particle to a plasma, is given in terms of the dielectric function by [9]

$$\frac{\partial E_a}{\partial t} = -\frac{2}{\hbar}\int \frac{d^3q}{(2\pi\hbar)^3}\hbar\omega n_B(\hbar\omega)V_{aa}(q)^2 \mathrm{Im}\,\varepsilon^{-1}(q,\hbar\omega). \tag{33}$$

Here n_b denotes the Bose function and V_{aa} is the Coulomb potential of the particle *a*. We observe that the sum about different plasma species is condensed in the dielectric function. It is noteworthy to remark that this result is valid for any arbitrary degeneracy. The derivation presented in [9] shows that the result (33) is more generally valid than has been derived earlier [10–12]. Higher-order correlations such as vertex corrections can be incorporated in the dielectric function, such that Eq. (33) remains valid [9]. This fact is important for dense solid-state plasmas which have been used recently for stopping experiments, where the result (33) is applicable as well. A more explicit form can be given by carrying out the angular integration $[q=\hbar k]$

$$\frac{\partial E_a}{\partial t} = \frac{2e_a^2}{\pi\varepsilon_0}\frac{1}{v(t)}\int_0^\infty \frac{dk}{k} \times \int_{-v(t)k+\hbar k^2/2m_a}^{v(t)k+\hbar k^2/2m_a} d\omega\,\omega n_B(\omega)\mathrm{Im}\,\varepsilon^{-1}(\hbar k,\omega). \tag{34}$$

Neglecting the quantum effects in Eq. (34) which represent an internal ionic cutoff due to the thermal de Broglie wavelength, we get the standard result of dielectric theory,

$$\frac{\partial E_a}{\partial t} = \frac{2e_a^2}{\pi\varepsilon_0}\frac{1}{v(t)}\int_0^\infty \frac{dk}{k}\int_0^{v(t)k} d\omega\ \omega\,\mathrm{Im}\,\varepsilon^{-1}(\hbar k,\omega), \tag{35}$$

from which all known special cases can be derived [9], among them the well-known Bethe formula. We use Eq. (34) where no artificial cutoff is needed further on.

In Fig. 3 we have plotted the stopping power of $^9Be^+$ calculated with the Mermin and the Lindhard dielectric functions. We observe that for a weakly coupled storage ring plasma with a temperature of 6 K and a density of 2.3×10^{13} m^{-3}, which corresponds to a nonideality of $\Gamma=0.13$, almost no differences are observed between the Mermin and Lindhard results. For higher coupling by lower temperature of 1 K corresponding to $\Gamma=0.77$, we see that the Mermin stopping power becomes smaller than the Lindhard result. Since the friction is dependent on the squared density but only on temperature via the Coulomb logarithm, we find a stronger dependence on the density. This is illustrated in Figs. 3–5. We see that with increasing density the deviations between the Mermin and Lindhard results become appreciable.

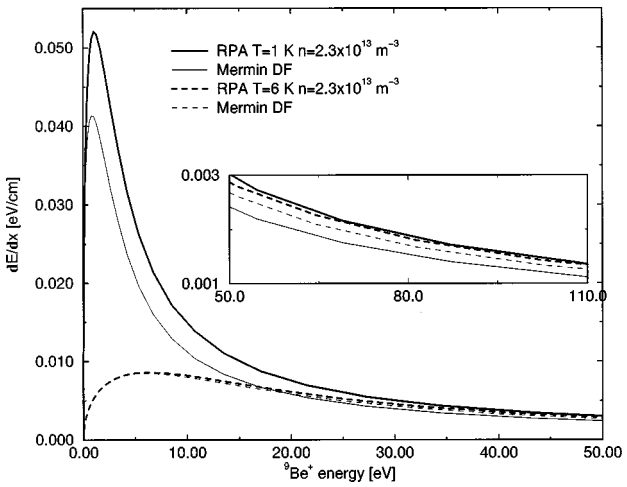

FIG. 3. The stopping power of $^9Be^+$ ions in an electronic plasma versus ion energy. The classical Lindhard result (thick lines) is compared with the Mermin result (thin lines) for two different temperatures. The plasma parameters are $\Gamma=0.77$ (solid lines) and $\Gamma=0.13$ (dashed lines), respectively.

So far we have generalized the dielectric theory of stopping power by the inclusion of collisions. It is instructive now to compare the results directly with the stopping power

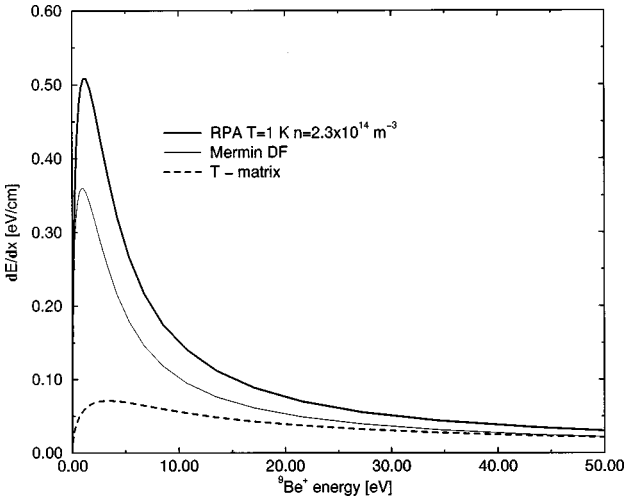

FIG. 4. The stopping power of $^9Be^+$ ions in an electronic plasma versus ion energy. The classical Lindhard result (thick line) is compared with the Mermin result (thin line) and the *T*-matrix result (dashed line) of binary collisions (36). The plasma parameter is $\Gamma=1.65$.

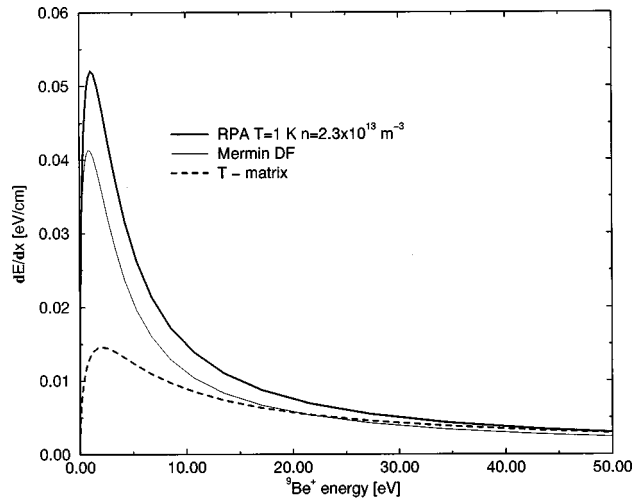

FIG. 5. Same situation as in Fig. 4, but lower density $\Gamma = 0.77$.

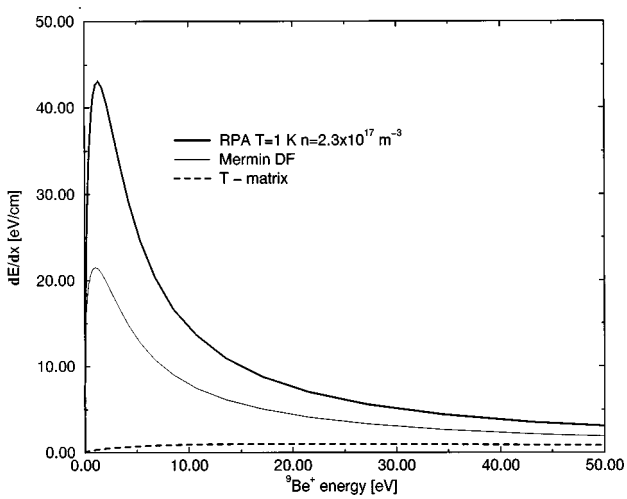

FIG. 6. Same as in Fig. 4, but density is now four orders of magnitudes higher ($\Gamma = 16.5$).

in the binary collision approximation. In [9] the following expression for the stopping power was derived from the Boltzmann equation within the *T*-matrix approximation:

$$\frac{\partial E}{\partial t}(v) = \sum_b \frac{n_b v_t}{m_b^2 \sqrt{\pi}} \frac{e^{-m_b v^2/2k_BT}}{v} \int_0^\infty dp\ p^2 \sigma_{ab}^t(p) \times \left[a \cosh a - \left(1 + \frac{p^2(1+m_b/m_a)}{m_a k_B T} \right) \sinh a \right] \times e^{-p^2/2m_b k_B T (1+m_b/m_a)^2} \tag{36}$$

with the thermal velocity $v_t^2 = 2k_BT/m_b$, the abbreviation $a = vp/k_BT(1+m_b/m_a)$, and the quantum-mechanical transport cross section

$$\sigma^t(p) = \int d\Omega\, (1 - \cos\,\theta) \frac{d\sigma}{d\Omega}. \tag{37}$$

In [13] a fit formula is given which subsumed the numerical results for the transport cross section for a plasma with charge $Z=1$. In Figs. 3–5 we compare the results for the dielectric theory of stopping power with and without collisional contributions with the pure two-particle collision result of Eq. (36). We see that the two-particle collision expression is significantly smaller than the dielectric theory. For very strong coupling in Fig. 6 we see even a vanishing contribution of the latter one indicating that the two-particle collisions do not contribute any more but the energy transfer is mainly caused by collective spreading. In Fig. 7 we represent the reduced energy loss $[\lambda_l = e^2/(12\pi\epsilon_0 T)]$

$$\frac{\lambda_l v_{\rm th}}{k_B T} \frac{1}{v} \frac{dE}{dx} \tag{38}$$

versus the coupling parameter $Z\Gamma^{3/2}$.

The dependence of the normalized energy loss from the coupling parameter is weaker in the Mermin case than in the RPA case but distinct from the numerical simulations. Nevertheless the involving of collisions modifies the stopping power in the right direction. The best description is still given by the *T*-matrix result (36).

B. Plasmons

The ion beam current $j(t)$ is a fluctuating quantity due to its granular (ionic) structure. Detecting the mirror charge on the vacuum chamber of the ring and Fourier transforming (frequency analyzing) one obtains the Schottky signal. It is primarily used for analyzing the beam's velocity distribution and hence the longitudinal temperature, but also important for measuring the particle number or the revolution frequency of the beam. It is related to the dynamical structure factor $S(\vec{q},\omega)$ by the equation [17]

$$\langle |J(q,\omega)|^2 \rangle \sim S(q,\omega), \tag{39}$$

where the angular brackets indicate the thermal averaging. The well-known fluctuation-dissipation theorem [18] con-

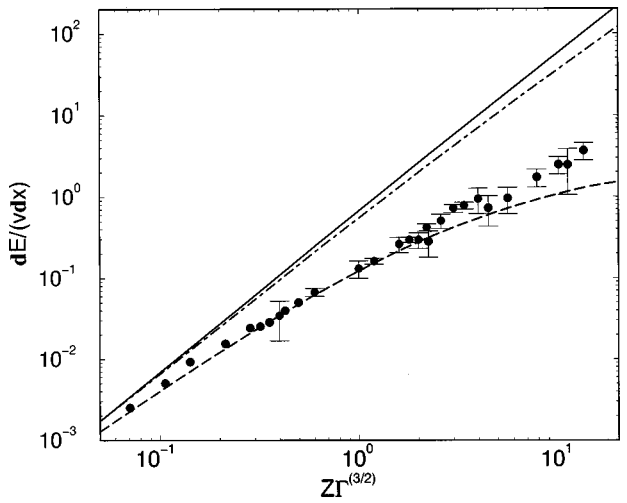

FIG. 7. The normalized friction coefficient (energy loss) for the RPA (solid line), the *T*-matrix result (dashed line), and the Mermin DF result (dot-dashed line). The filled circles are simulation results [14] which reproduce experimental data [15,16].

nects the imaginary part of the response function Im $\epsilon(\vec{q},\omega)$ and the dynamical structure factor

$$S(\vec{q},\omega) = -\frac{k_B T}{\omega V_C(\vec{q})} \,\mathrm{Im}\, \epsilon^{-1}(\vec{q},\omega)$$

with the Coulomb potential V_C. In dense ion beams (e.g., the C^{6+} LIR experiment) one observes a double-peaked Schottky spectrum. The two peaks commonly identified as plasma waves propagate in two directions around the storage ring. A frequency analysis of this beam current shows the propagating waves clearly as peaks in the spectra which are theoretically well described in [3,8]. We now use the identity of the Mermin and VFP dielectric functions to compute the Schottky noise much easier within the Mermin DF.

For numerical calculation one has to modify the plasma frequency, which differs from that of an isotropic plasma. For a plasma in a conducting tube we have [8]

$$\tilde{\omega}_{\mathrm{pl}}^2 = \frac{NZ^2e^2M}{2\pi R_0^3 m \epsilon_0}\left(\ln\frac{r_C}{r_B} + \frac{1}{2}\right). \tag{40}$$

Here N denotes the particles number, r_C the radius of the beam chamber, r_B the radius of the beam, $2\pi R_0$ is the circumference of the ring, and M is the number of plasma waves fitting in the ring, the so-called harmonic wave number. We assume for simplicity the nonrelativistic case, which is valid in the TSR experiments ($^9Be^+$: $0.04c$, $^{12}C^{6+}$: $0.15c$) with $\gamma \approx 1$.

The wavelength q is not a continuous variable but assumes only discrete values $q = M/2\pi R_0$. The fraction κ^2/q^2 can now be expressed by

$$\frac{\kappa^2}{q^2} = 2\frac{\tilde{\omega}_{\mathrm{pl}}^2}{\delta\omega^2} \tag{41}$$

with the thermal frequency

$$\delta\omega^2 = \frac{2k_B T}{R_0^2 m}. \tag{42}$$

Inserting these parameters into the VFP dielectric function, one obtains

$$\epsilon_{\mathrm{VFP}}(M,\omega) = 1 + 2\left(\frac{\tilde{\omega}_{\mathrm{pl}}}{\delta\omega}\right)^2 \times {}_1F_1\left(1,1 + \frac{M^2\delta\omega^2}{2\lambda^2} - \frac{i\omega}{\lambda}, \frac{M^2\delta\omega^2}{2\lambda^2}\right). \tag{43}$$

This is the well-known standard permittivity in the Schottky noise theory. Since the Mermin DF and the VFP DF are identical, it is more practical to use the easier Mermin DF. We modify Eq. (24) according to the parameters (40)–(42),

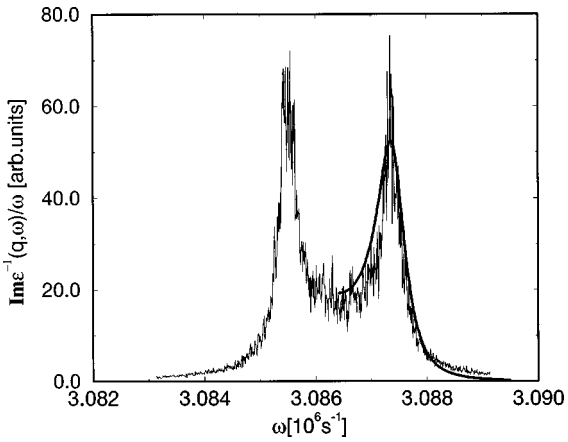

FIG. 8. The Schottky spectra of a dense carbonium beam and the corresponding theoretical prediction. ($n = 8.3\times10^{13}$ m^{-3}, $T_\parallel = 11\,000$ K.) Data are taken from [19].

$$\epsilon_{\mathrm{M}}(M,\omega+i\lambda) = 1 + \frac{\left(1+\frac{i\lambda}{\omega}\right)[\epsilon(M,\omega+i\lambda)-1]}{1+\frac{i\lambda}{\omega}\,\frac{\epsilon(M,\omega+i\lambda)-1}{\epsilon(M,0)-1}} \tag{44}$$

with Eq. (17) for $\epsilon(M,\omega+i\lambda)$ and

$$\epsilon_{\mathrm{M}}(M,0) = 1 + 2\frac{\tilde{\omega}_{\mathrm{pl}}^2}{\delta\omega^2}. \tag{45}$$

In the next step we insert a relaxation time considering the anisotropy in the thermal velocities v_{th} [5],

$$\lambda = 4\pi(Ze)^4 \frac{n}{\epsilon^2 m^2 v_{\mathrm{th},\perp} v_{\mathrm{th},\parallel}^2}\Lambda. \tag{46}$$

Here Λ again denotes the Coulomb logarithm. We have used the modified Mermin dielectric function for calculating the plasmonic excitation for a $^{12}C^{6+}$ beam at an energy of 73.3 MeV and a revolution frequency of $v_0/R_0 = 617$ kHz ($M = 5$). In (see Fig. 8) the expression Im $\epsilon(M,\omega)/\omega$ is compared with the Schottky measurement. We see that the modified Mermin dielectric function fits the Schottky spectra satisfactorily.

IV. SUMMARY

In this paper we have described two dielectric functions including collisions. After numerical inspection we have shown that the DF obtained from the VFP equation is identical to the Mermin DF. Modifying the dielectric function for storage ring purposes (modified plasma frequency, discrete wave numbers or harmonics) we have derived the standard dielectric function for Schottky noise prediction for a three-dimensional plasma beam. Because of the identity of both dielectric functions, one can use a Mermin dielectric function for Schottky noise description, too. The second goal was a better description of the stopping power acting on an ion beam in the cooler's electron gas. Here we would like to state that including the collisions leads to a lower friction force than in the RPA predictions but obviously overesti-

mates the friction force compared with simulated and experimental results.

Further improvement has to be done to consider strong-coupling effects in the relaxation time by using a matching Coulomb logarithm. Efforts have also to be made to include the magnetic field in the cooler and the anisotropic Maxwell distributions in the dielectric function.

ACKNOWLEDGMENTS

The authors acknowledge stimulating discussions with G. Röpke (Rostok), A. Wolf, M. Grieser, and M. Beutelspacher (TSR Group, Heidelberg). This work was supported from the BMBF (Germany) under Contract No. 06R0884, and the Max Planck Society.

APPENDIX A: SOLUTION OF THE VLASOV-FOKKER-PLANCK EQUATION

We are following the main ideas of [20]. At first we introduce the reduced variables

$$\vec{u}=\sqrt{\frac{m}{2k_BT}}\vec{v},\quad \vec{k}=\frac{\vec{q}}{\lambda}\sqrt{\frac{k_BT}{2m}}. \tag{A1}$$

After linearization of the VFP equation (25), we arrive at

$$\frac{\partial}{\partial t}\delta f(\vec{k},\vec{u},t)+2i\lambda\vec{u}\cdot\vec{k}\delta f(\vec{k},\vec{u},t)-\frac{2i\lambda}{m}\vec{k}\cdot U(\vec{k},t)\frac{\partial f_0(\vec{u})}{\partial\vec{u}}$$
$$=\lambda\frac{\partial}{\partial\vec{u}}\left(\frac{1}{2}\frac{\partial}{\partial\vec{u}}+\vec{u}\right). \tag{A2}$$

For the Fokker-Planck term including the second term of the left side (the so-called inhomogeneous Fokker-Planck operator), one can consider the eigenvalue and eigenfunctions in three dimensions,

$$\left[-2i\lambda\vec{u}\cdot\vec{k}+\lambda\frac{\partial}{\partial\vec{u}}\cdot\left(\frac{1}{2}\frac{\partial}{\partial\vec{u}}+\vec{u}\right)\right]\psi_{n_xn_yn_z}(\vec{k},\vec{u})$$
$$=\Lambda_{n_xn_yn_z}(\vec{k})\psi_{n_xn_yn_z}(\vec{k},\vec{u}). \tag{A3}$$

The eigenfunctions take the form after a coordinate transformation $z=u+2ik$,

$$\psi_{n_xn_yn_z}=\sqrt{\frac{1}{n_x!n_y!n_z!2^{n_x+n_y+n_z}}\left(\frac{m}{2\pi k_BT}\right)^3}$$
$$\times e^{k^2}e^{-(\vec{z}-i\vec{k})^2}H_{n_x}(z_x)H_{n_y}(z_y)H_{n_z}(z_z). \tag{A4}$$

One can identify the functions H_n as Hermite polynomials. The lowest eigenfunction for $n_x=n_y=n_z=0$ is the Maxwell distribution. The eigenvalues are

$$\Lambda_{n_xn_yn_z}=-\lambda(n_x+n_y+n_z+2k^2). \tag{A5}$$

In the next step we insert for the right side the eigenvalues and eigenfunctions of the inhomogeneous Fokker-Planck operator

$$\frac{\partial}{\partial t}\delta f(\vec{k},\vec{u},t)-\frac{2i\lambda}{m}\vec{k}\cdot U(\vec{k},t)\frac{\partial f_0(\vec{u})}{\partial\vec{u}}=\lambda\sum_{n_xn_yn_z}\mu_{n_xn_yn_z}\psi_{n_xn_yn_z} \tag{A6}$$

with

$$\mu_n(\vec{k})=\frac{\Lambda_n(\vec{q})}{\lambda}$$

and expand the distribution function $(\partial/\partial\vec{u})f_0$ and the distortion $\delta f(\vec{u},\vec{k},t)$ in a sum of eigenfunctions of the Fokker-Planck operator

$$\vec{k}\frac{\partial}{\partial\vec{u}}f_0(\vec{u})=\vec{k}\cdot\sum_{n_xn_yn_z}^{\infty}\vec{a}_{n_xn_yn_z}\psi_{n_xn_yn_z}(\vec{u},\vec{k}),$$
$$\delta f(\vec{u},\vec{k},t)=\sum_{n_xn_yn_z}^{\infty}c_{n_xn_yn_z}\psi_{n_xn_yn_z}. \tag{A7}$$

Performing a Fourier transformation $t\to\omega$ we arrive at a solution for the coefficients

$$c_{n_xn_yn_z}=\frac{\frac{i\lambda}{k_BT}\vec{k}\cdot\vec{a}_nU(\vec{k},\omega)}{-i\omega-\lambda(n_x+n_y+n_z+2k^2)}. \tag{A8}$$

Remembering Eq. (15), we obtain

$$\delta n(\vec{k},\omega)=\sum_{n_xn_yn_z}c_{n_xn_yn_z}\int_{\rm vol}\psi_{n_xn_yn_z}d^3u \tag{A9}$$
$$=U(\vec{k},\omega)\Pi_{\rm VFP}(\vec{k},\omega).$$

Hence we get for the polarizability

$$\Pi_{\rm VFP}(k,\omega)=\frac{\lambda}{2\pi k_BT}\exp[k^2]\sum_{n_xn_yn_z}i^{2(n_x+n_y+n_z)}\frac{\Gamma(\frac{1}{2}+n_x)\Gamma(\frac{1}{2}+n_y)\Gamma(\frac{1}{2}+n_z)\Gamma(\frac{1}{2}+n_x+n_y)}{n_x!n_y!n_z!(n_x+n_y)!(n_x+n_y+n_z)!}$$
$$\times\frac{(n_x+n_y+n_z+2k^2)(\sqrt{2}k)^{2(n_x+n_y+n_z)}}{-i\omega-\lambda(n_x+n_y+n_z+2k^2)}. \tag{A10}$$

Using the relations

$$\sum_{n_x,n_y,n_z} \frac{\Gamma(\frac{1}{2}+n_x)\Gamma(\frac{1}{2}+n_y)\Gamma(\frac{1}{2})+n_z)\Gamma(\frac{1}{2}+n_x+n_y)}{n_x!n_y!n_z!(n_x+n_y)!(n_x+n_y+n_z)!} = \sum_m \frac{\pi^2}{m!} \tag{A11}$$

and

$$\sum_n^{\infty} \frac{(-x)^n}{n!(\kappa+n)} = \frac{\exp[-x]}{\kappa} {}_1F_1(1,1+\kappa,x) \tag{A12}$$

we arrive finally at

$$\Pi_{\mathrm{VFP}}(k,\omega) = \frac{\pi}{2k_BT}\left[1+\frac{i\omega}{2\lambda k^2 - i\omega} {}_1F_1\left(1,1+2k^2-i\frac{\omega}{\lambda};2k^2\right)\right]. \tag{A13}$$

The dielectric function related to this polarizability was discussed in Sec. II B.

[1] D. Habs and R. Grimm, Annu. Rev. Nucl. Part. Sci. **45**, 391 (1995).
[2] H. Poth, Phys. Rep. **196**, 135 (1990).
[3] V. Parkhomchuk and D. Pestrikov, Zh. Tekh. Fiz. **50**, 1411 (1980) [Sov. Phys. Tech. Phys. **25**, 818 (1980)].
[4] U. Schramm, Hyperfine Interact. **108**, 273 (1997).
[5] A. H. Sørensen, in *CERN Accelerator School*, edited by S. Turner (CERN, Geneva, 1987).
[6] G. Röpke and A. Wierling, Phys. Rev. E **57**, 7075 (1998).
[7] N. D. Mermin, Phys. Rev. B **1**, 2362 (1970); K. L. Kliewer and R. Fuchs, Phys. Rev. **181**, 552 (1969).
[8] V. A. Lebedev, J. S. Hangst, and J. S. Nielsen, Phys. Rev. E **52**, 4345 (1995).
[9] K. Morawetz and G. Röpke, Phys. Rev. E **54**, 1 (1996).
[10] W. D. Kraeft and B. Strege, Physica A **149**, 313 (1988).
[11] H. H. Brouwer *et al.*, Contrib. Plasma Phys. **30**, 263 (1990).
[12] H. H. Brouwer *et al.*, Contrib. Plasma Phys. **30**, 369 (1990).
[13] G. Röpke and R. Redmer, Phys. Rev. A **39**, 907 (1989).
[14] G. Zwicknagel, C. Toepffer, and P. Reinhard, Hyperfine Interact. **99**, 285 (1996).
[15] A. Wolf *et al.*, *Proceedings of the Workshop on Beam Cooling and Related Topics, Montreux, 1993* (CERN, Geneva, 1994), p. 416.
[16] T. Winkler *et al.*, Hyperfine Interact. **99**, 277 (1996).
[17] V. Avilov and I. Hofmann, Phys. Rev. E **47**, 2019 (1993).
[18] R. Kubo, J. Phys. Soc. Jpn. **12**, 570 (1957).
[19] K. Tetzlaff, diploma thesis, Max Planck Institute for Nuclear Physics, 1997 (unpublished).
[20] P. Resibois and M. de Leener, *Classical Kinetics Theory of Fluids* (Wiley, New York, 1977), p. 41.